Cell Reports
Physical Science

Article

Elastic remodeling of model and cell membranes by rotating ATP synthase

Graphical abstract

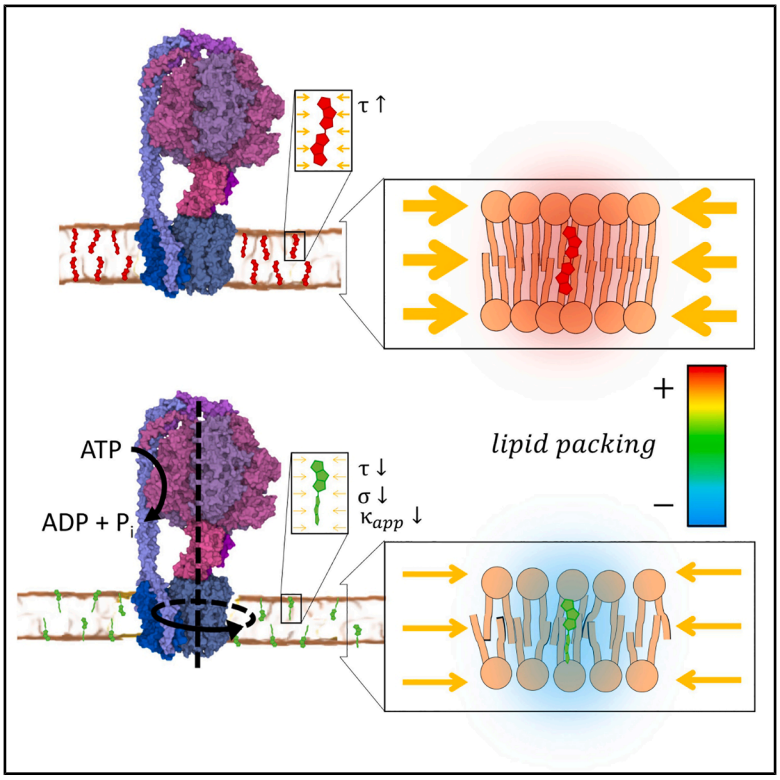

Authors

David Valdivieso González,
Miguel A. Sacristán, Paolo Natale,
Belén Orgaz, M. Pilar Lillo,
Víctor Almendro-Vedia,
Iván López-Montero

Correspondence

ivanlopez@quim.ucm.es

In brief

ATP synthase is a transmembrane molecular rotor that synthesizes ATP by harnessing the energy from the proton flow across the embedding membrane. Now, Valdivieso González et al. provide direct insights into the impact of protein rotation on membrane rigidity, tension, and lipid packing in both model and living bacterial membranes.

Highlights

- ATP synthase rotation reduces lipid packing, lowering membrane tension in giant vesicles
- Membrane flexibility increases as lateral pressure drops due to ATP synthase activity
- Stimulated ATP synthase activity lowers lateral pressure of *B. subtilis* plasma membranes

Valdivieso González et al., 2025, Cell Reports Physical Science 6, 102567
May 21, 2025
https://doi.org/10.1016/j.xcrp.2025.102567

CellPress

Cell Reports
Physical Science

CellPress
OPEN ACCESS

Article

Elastic remodeling of model and cell membranes by rotating ATP synthase

David Valdivieso González,[1,2,3] Miguel A. Sacristán,[1,2,3] Paolo Natale,[1,2,3] Belén Orgaz,[3,4] M. Pilar Lillo,[5] Víctor Almendro-Vedia,[2,3,4] and Iván López-Montero[1,2,3,6,*]

[1]Departamento Química Física, Universidad Complutense de Madrid, Avenida Complutense s/n, 28040 Madrid, Spain
[2]Instituto de Investigación Sanitaria Hospital Doce de Octubre (imas12), Avenida de Córdoba s/n, 28041 Madrid, Spain
[3]Instituto Pluridisciplinar, Paseo Juan XXIII, 1, 28040 Madrid, Spain
[4]Sección Departamental de Farmacia Galénica y Tecnología Alimentaria, Facultad de Veterinaria, Universidad Complutense de Madrid, Avenida Complutense s/n, 28040 Madrid, Spain
[5]Departamento Química Física Biológica, Instituto de Química-Física "Blas Cabrera" (CSIC), Serrano 119, 28006 Madrid, Spain
[6]Lead contact
*Correspondence: ivanlopez@quim.ucm.es
https://doi.org/10.1016/j.xcrp.2025.102567

SUMMARY

Energy homeostasis in cells relies on the rotary motion of ATP synthase. The spinning movement is also assumed to impact the mechanical properties of the surrounding lipids, leading to emergent effects such as non-equilibrium membrane fluctuations or protein curvature sorting in model systems. Here, we demonstrate that ATP synthase rotation reduces lateral pressure by decreasing lipid packing in both artificial and bacterial membranes. Using micropipette aspiration and fluorescence lifetime imaging microscopy, we find that the rotation of ATP synthase lowers the membrane tension of giant unilamellar vesicles, making the membranes more flexible. Fluorescent probes sensitive to lipid packing confirm that ATP synthase lowers membrane surface pressure during rotation. *In vivo* experiments in *Bacillus subtilis* further reveal that stimulation of ATP synthase rotation with specific drugs decreases the lateral pressure of the plasma membrane. These findings suggest that ATP synthase plays a significant role in modulating the mechanical properties of native membranes, potentially driving biological processes linked to membrane dynamics and protein self-assembly.

INTRODUCTION

F_1F_o-ATP synthase (adenosine triphosphate [ATP] synthase) is an evolutionarily conserved multiprotein complex that plays a key role in producing ATP, the cell's main energy source. The enzyme consists of two functional domains: the hydrophilic F_1 domain, which contains the catalytic head and a central stalk, and the hydrophobic F_o domain, composed of the peripheral stalk and a membrane-embedded region. The membrane portion of the F_o domain includes a *c*-ring oligomer that rotates in response to either a proton (ΔpH) or an electrochemical gradient ($\Delta\Psi$) across the membrane.[1,2] Notably, the *c*-ring can rotate in both clockwise and counterclockwise directions, depending on whether the enzyme is synthesizing or hydrolyzing ATP. During ATP synthesis, protons move across the membrane fueled by the electrochemical gradient causing the *c*-ring to rotate. This motion is then transferred to the central stalk, inducing conformational changes in the F_1 catalytic sites. These changes allow adenosine diphosphate (ADP) and inorganic phosphate (P_i) to bind, resulting in the release of newly synthesized ATP. In the ATP hydrolysis operating mode, the catalytic head breaks down ATP into ADP and P_i, reversing the *c*-ring's rotation and actively pumping protons against the gradient, thereby regulating the proton motive force.[3,4]

The rotary motion of the *c*-ring not only drives the synthesis and hydrolysis of ATP but also generates membrane-mediated effects that impact the biophysical properties of the surrounding lipid bilayer. This active rotary activity induces non-equilibrium fluctuations in the lipid bilayers,[5] as detected by a decrease in both the membrane tension and the bending properties of the embedding membrane. The enhanced fluctuations were hypothesized to promote an active protein clustering into mechanical hot spots characterized by a high curvature. Indeed, the rotary motion was shown later to play a key role in the active curvature sorting of monomeric ATP synthase into lipid filaments.[6] Although the effects of ATP synthase's rotary motion on membrane dynamics have been observed, the molecular mechanisms underlying these processes remain unknown. The current evidence through molecular dynamics simulations suggests that the rotation of the *c*-ring induces changes in the local structure of the lipid membrane, potentially altering lipid packing and membrane thickness.[6] However, despite these observations, direct experimental evidence linking the rotary movement of ATP synthase to specific alterations in membrane lipid structure is still lacking.

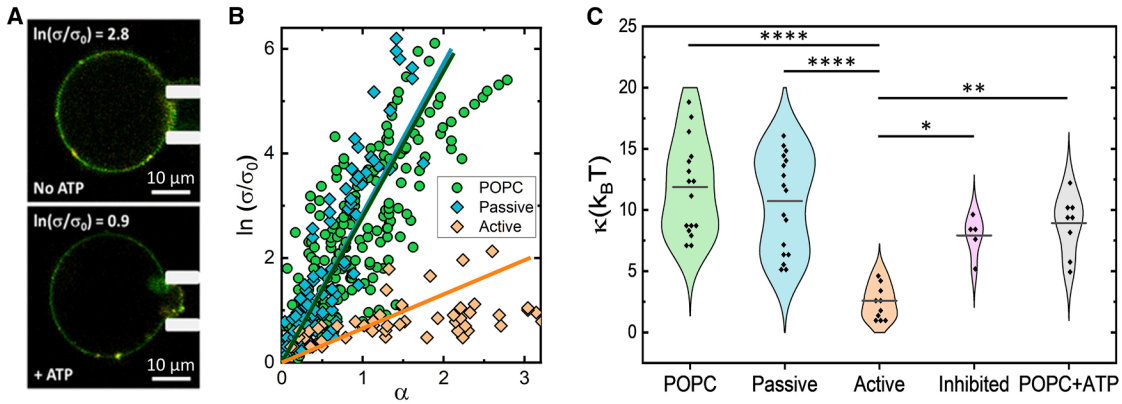

Figure 1. Micropipette aspiration of GUVs and proteoGUVs (ATP synthase)

(A) Confocal micrographs of a GUV aspirated in a micropipette at medium (top) and low (bottom) tension for proteoGUVs in passive and active conditions, respectively (membrane in green, ATP synthase in red). The change in the length of the protrusion is proportional to the change in the relative excess area. Scale bars, 10 μm.

(B) Plot of the logarithm of the relative tension (σ/σ_0) versus the relative excess area α for different pure POPC GUVs and proteoGUVs containing ATP synthase in the absence (passive) and presence (active) of ATP.

(C) Violin plot comparing the bending modulus distribution for POPC GUVs ($12 \pm 4\ k_BT$, $N = 16$); proteoGUVs containing ATP synthase under passive (11 ± 4, $N = 17$), active (3 ± 1, $N = 10$), and inhibited conditions ($8 \pm 3\ k_BT$, $N = 5$); and POPC GUVs in the presence of ATP ($9 \pm 3\ k_BT$, $N = 8$). Mean values are expressed as the mean ± SD for N independent measurements. The mean is represented by a line. Statistical significance: $^*p \leq 0.05$, $^{**}p \leq 0.01$, $^{***}p \leq 0.001$, and $^{****}p \leq 0.0001$.

In this study, we provide direct measurements of the effects that ATP synthase's rotary motion produces on membrane mechanics. Using micropipette aspiration,[7] we observed a decrease in the surface tension of lipid membranes reconstituted with active ATP synthase, demonstrating that the enzyme's rotational movement enhances membrane flexibility. This was further confirmed with a fluorescent membrane tension probe,[8] which allowed us to visualize changes in membrane packing in both a reconstituted system—using ATP synthase from *Escherichia coli* in giant unilamellar vesicles (GUVs)—and bacterial biomembranes. The results offer definitive evidence that ATP synthase's rotation decreases lateral pressure within the lipid bilayer, effectively reducing lipid lateral packing. These findings confirm that the rotary motion of ATP synthase actively modulates membrane elasticity, providing key insights into how this molecular motor influences membrane structure and dynamics in native biomembranes.

RESULTS

Rotating ATP synthase decreases the membrane tension of lipid bilayers

We have previously measured a decrease in the bending modulus in GUVs composed of an *E. coli* lipid extract containing the ATP synthase and in the presence of ATP.[5] Analyzing the shape fluctuations or normal undulations of quasi-spherical GUVs,[9] we found that the ATP synthase promoted large non-equilibrium deformations at particular sites of the membrane, and the bending modulus was reduced by a factor ≈ 4.[5] Here, the bending modulus of 1-palmitoyl-2-oleoyl-sn-glycero-3-phosphocholine (POPC) GUVs containing ATP synthase in the presence and in the absence of ATP was measured by micropipette aspiration[7] (see methods). The micropipette instrument exploits the Canham-Helfrich equation, which connects the relative excess area, $\alpha = \frac{A-A_0}{A_0} = \frac{\Delta A}{A_0}$, and the membrane tension σ by:

$$\sigma \approx \sigma_0 \exp\left(\frac{8\pi\kappa\alpha}{k_BT}\right) + K\alpha \qquad \text{(Equation 1)}$$

where σ_0 is the lowest membrane tension required to hold the vesicle, κ is the bending modulus of the vesicle, k_BT is the thermal energy, and K is the stretching modulus of the membrane. In a typical suction experiment, a GUV is seized and pulled out by a cylindrical micropipette in the aspiration mode, where the pressure difference between the vesicle interior and the pipette determines both σ and α (Figure 1A). κ is obtained from the fitting of Equation 1 to the experimental data in the low-deformation regime (Figure 1A). A first set of experiments provided the bending modulus of pure lipid vesicles made of POPC (Figure 1B), $\kappa_l = 12 \pm 4 k_BT\ (N = 16)$. This value is in agreement with previously reported measurements for POPC.[10] As expected for a low-yield reconstitution, the ATP synthase did not alter the stiffness of the membrane, $\kappa_{Passive} = 11 \pm 4 k_BT\ (N = 17)$ (Figure 1B). Remarkably, the bending modules decreased to $\kappa_{Active} = 3 \pm 1 k_BT\ (N = 10)$ upon ATP incubation (Figure 1C). Additional controls were run, first incubating simultaneously with ATP and the specific inhibitor N,N′-dicyclohexylcarbodiimide (DCCD; 1 mM final concentration). DCCD binds covalently to the *c*-ring in F_o and thereby blocks its rotation.[11,12] Under this inhibitory condition, the bending modulus was similar to that measured in the absence of ATP, $\kappa^{ATP}_{DCCD} = 8 \pm 3\ k_BT\ (N = 5)$ (Figure 1C). Finally, we also measured the bending modulus of POPC GUVs in the presence of ATP, obtaining a bending rigidity of $\kappa^{ATP}_{POPC} = 9 \pm 3\ k_BT\ (N = 8)$ (Figure 1C). The observed membrane softening under rotating conditions was then compatible with a change in the lipid packing of the embedding membrane.

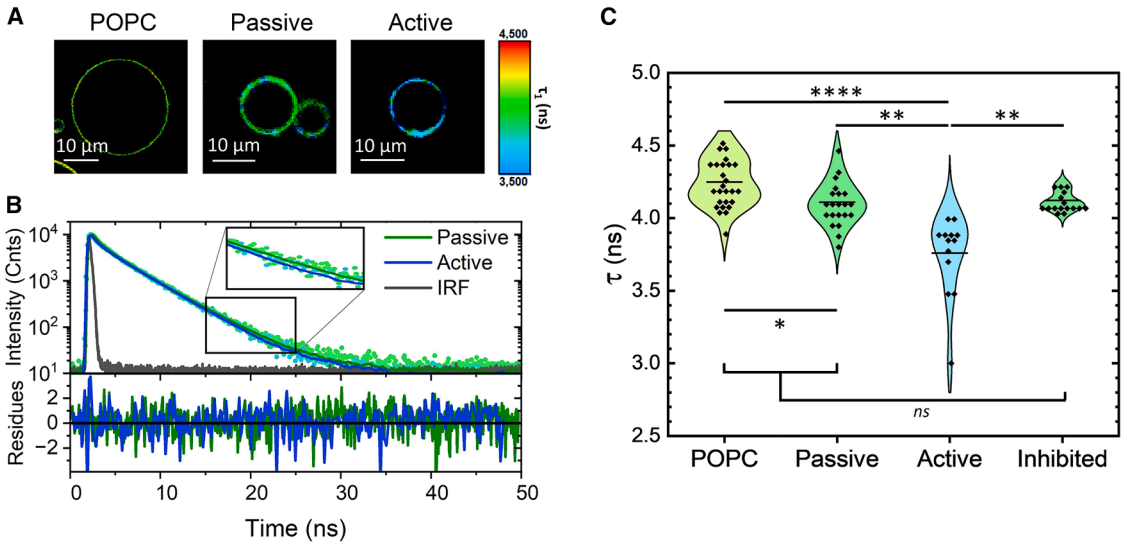

Figure 2. FLIM of GUVs and proteoGUVs (ATP synthase) using the Flipper-TR membrane tension probe

(A) Fluorescence lifetime imaging (τ_1) of representative pure POPC GUVs and proteoGUVs containing ATP synthase in the absence (passive) and presence (active) of ATP. Scale bars, 10 µm.

(B) Typical fluorescence lifetime decay of passive (green) and active GUVs (blue).

(C) Violin plot of Flipper-TR lifetime τ_1 for different pure POPC GUVs (4.2 ± 0.2 ns, $n = 26$) and proteoGUVs containing ATP synthase under passive (4.1 ± 0.2 ns, $n = 26$), active (3.8 ± 0.3 ns, $n = 13$), and inhibited conditions (4.1 ± 0.1 ns, $n = 16$). The mean is represented by a line. Mean values are expressed as the mean ± SD from n field of views. Statistical significance: *ns* ($p > 0.05$), *$p \leq 0.05$, **$p \leq 0.01$, ***$p \leq 0.001$, and ****$p \leq 0.0001$.

Membrane packing modulation by ATP synthase rotation activity

To correlate the decrease in membrane surface tension observed in the micropipette aspiration experiments with changes in the lipid packing, we ran independent measurements using a fluorescent membrane tension probe.[8] Flipper-TR probes contain two planar push-pull fluorophores connected by a flexible linker that responds to mechanical forces within the membrane. The key outcome of the flipper-based probes is a change in fluorescence lifetime, which is highly sensitive to variations in lateral pressure and membrane packing. Under conditions of low lipid lateral packing, the probe remains in a twisted conformation, resulting in a small fluorescence lifetime. However, when the membrane experiences tighter lipid packing, the probe adopts a planar conformation, causing an upshift in its fluorescence lifetime.

We first measured the lifetime of Flipper-TR by fluorescence lifetime imaging microscopy (FLIM) in pure POPC GUVs and proteoGUVs (Figure 2A), which were externally supplemented with the tension probe (1 µM final concentration). A detailed global analysis of the time-resolved decays by a multiexponential function revealed the existence of three lifetimes in all conditions (Figure 2B). The shortest lifetime, $\tau_3 \approx 0.3$ ns, with a slight contribution and a low fractional intensity ($f_3 < 0.1$), was ascribed to the experimental background (see methods for more details). As previously reported, the fractional intensity f_2 of the second lifetime, ($f_2 = 0.2 \pm 0.1$), was significantly lower than the fractional intensity f_1 of the longest lifetime, ($f_1 = 0.7 \pm 0.1$). From now on, we use τ_1 as a reliable descriptor to monitor the changes in membrane packing produced by protein activity, as τ_2 is more sensitive to errors.[8]

As expected, the lifetime $\tau_1 = 4.3 \pm 0.2$ ns ($N = 237$ GUVs from $n = 26$ images) of Flipper-TR in POPC GUVs presented intermediate lifetime values relative to 1,2-dioleoyl-sn-glycero-3-phosphocholine (DOPC) and DOPC:Cholesterol GUVs[8] (Figure S1). Similar measurements were then performed in proteoGUVs containing ATP synthase in both the presence and the absence of ATP, termed as active and passive conditions, respectively. A first set of measurements showed a small decrease in τ_1 in the presence of ATP synthase compared to bare POPC GUVs, $\tau_1^{Passive} = 4.1 \pm 0.1$ ns ($N = 126$ GUVs from $n = 26$ images). Remarkably, with the addition of ATP, i.e., under rotating conditions, τ_1 decreased significantly, $\tau_1^{Active} = 3.8 \pm 0.3$ ns ($N = 39$ GUVs from $n = 13$ images) (Figure 2C). In inhibited conditions, i.e., in the presence of ATP and DCCD, τ_1 remained similar to the lifetime for passive conditions, $\tau_1^{Inhibited} = 4.1 \pm 0.1$ ns ($N = 33$ GUVs from $n = 16$ images) (Figure 2C). Since DCCD treatment does not fully inhibit F_oF_1 activity and has little effect on the ATPase activity of ATP synthase in a decoupled state,[6] we conducted an additional control experiment using proteoGUVs in the presence of ADP (1 mM). The resulting lifetimes were similar to those observed for POPC vesicles and passive conditions, $\tau_1^{ADP} = 4.4 \pm 0.1$ ns ($N = 26$ GUVs from $n = 15$ images) (Figure S2). Finally, the effect of ATP on POPC GUVs was also assessed, obtaining lifetimes similar to those of pure POPC vesicles in the absence of nucleotide, $\tau_1^{POPC+ATP} = 4.5 \pm 0.2$ ns ($N = 80$ GUVs from $n = 19$ images) (Figure S3). Along with the findings from micropipette aspiration experiments (Figure 1), the shortened fluorescence lifetime of the probe demonstrates a detectable decrease in lipid packing and membrane lateral pressure by the rotating movement of ATP synthase.

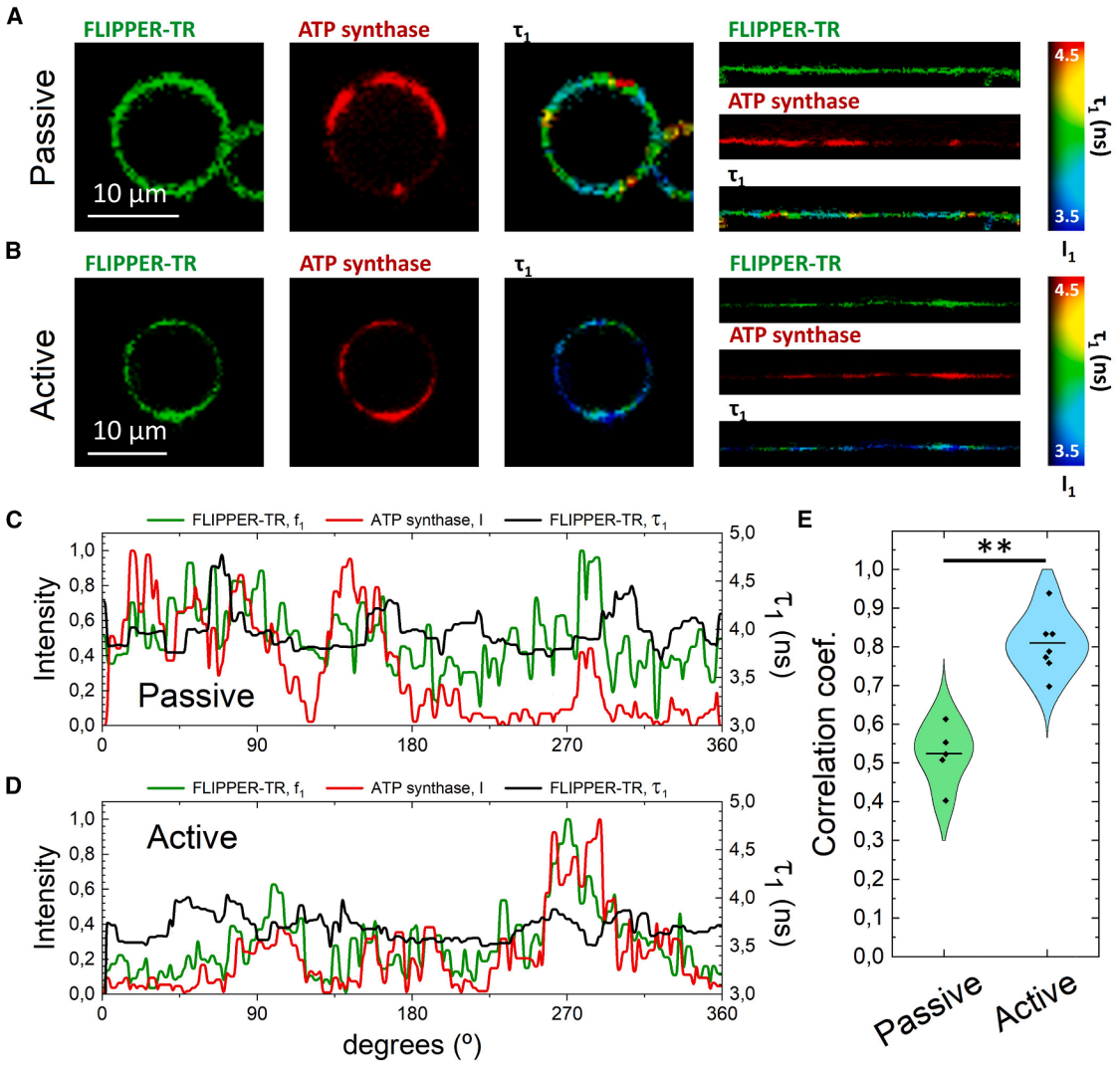

Figure 3. Spatial correlation of ATP synthase and Flipper-TR

(A and B) Fluorescence intensity of both the probe (green channel, f_1) and ATP synthase (red channel, *I*) along the membrane contour of typical proteoGUVs in passive (A) and active (B) conditions and the probe's lifetime (τ_1). Scale bars, 10 µm.

(C and D) Fluorescence intensity values (f_1) of both the probe (green channel) and ATP synthase (red channel, *I*) along the membrane contour of typical proteoGUVs in passive (C) and active (D) conditions.

(E) Violin plot of the correlation coefficient between the fluorescence intensity of Flipper-TR and the ATP synthase intensity for passive ($r_{Passive} = 0.53 \pm 0.08, N = 5$) and active conditions ($r_{Active} = 0.83 \pm 0.06, N = 7$). The mean is represented by a line. Mean values are expressed as the mean ± SD from *N* vesicles. Statistical significance: $^{**}p \leq 0.01$.

Interaction of Flipper-TR with ATP synthase

The slight decrease in τ_1 due to the presence of ATP synthase (Figure 2C), while bending stiffness remains unchanged (Figure 1C), suggests a specific enzyme-probe interaction that may alter the fluorophore's photophysics, creating an apparent lipid packing reduction. To quantify this effect in active conditions and confirm that ATP synthase's rotational motion reduces the lateral pressure of the embedding lipid bilayer, we compared the spatial distribution between the fluorescent probe and ATP synthase within proteoGUVs. For this, proteoGUVs were built with previously labeled ATP synthases with Alexa 555. A first analysis considered the spatial correlation between ATP synthase and Flipper-TR based on the fluorescence intensities in both passive and active conditions (Figures 3A and 3B). Unlike pure POPC vesicles, which presented a homogeneous distribution of the probe along the membrane (Figure S4), proteoGUVs sometimes displayed areas of the membrane with a higher protein concentration that was accompanied by a concomitant accumulation of the probe (Figures 3C and 3D). The spatial correlation of fluorescence intensities confirmed a significant association between ATP synthase and the tension probe in both passive ($r_{Passive} = 0.53 \pm 0.08, N = 5$) and active ($r_{Active} = 0.83 \pm 0.06, N = 7$) conditions (Figure 3E).

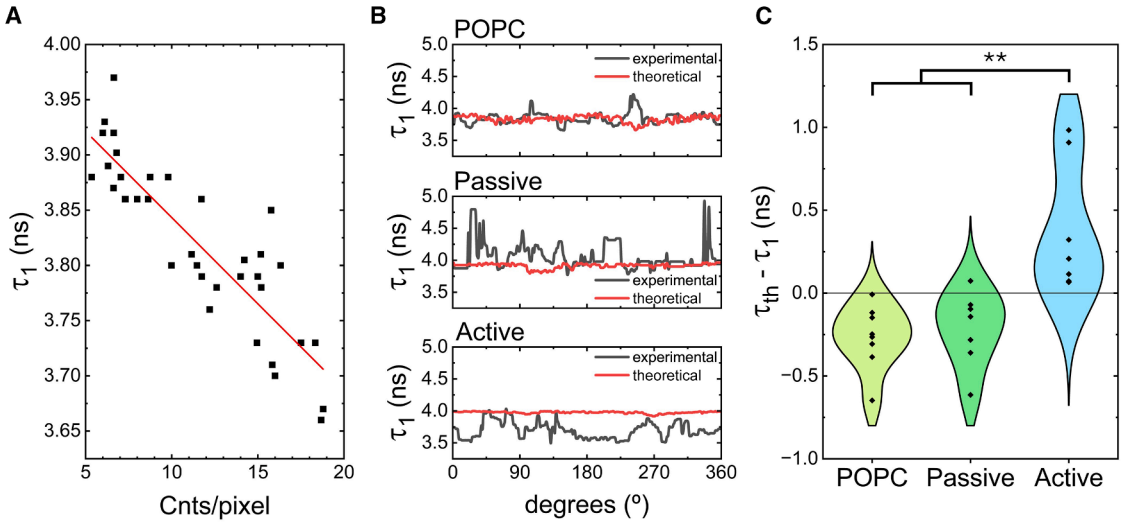

Figure 4. Concentration effects on the lifetime of Flipper-TR

(A) Lifetime of Flipper-TR as a function of the probe concentration on supported lipid bilayers (SLBs) made of POPC. Linear fit: $\tau_1 = m \cdot \frac{Cnts}{pixel} + b$, where $m = -0.016$ and $b = 3.999$.

(B) Experimental (black) and theoretical (red) lifetimes measured along representative POPC GUVs and proteoGUVs under passive and active conditions. τ_{th} is calculated for every pixel along vesicle contours using the linear fit in (A).

(C) Violin plot of $\tau_{th} - \tau_1$ for POPC GUVs ($N = 9$) and proteoGUVs under passive ($N = 7$) and active conditions ($N = 7$). Statistical significance: $^{**}p \leq 0.01$.

A high local concentration of Flipper-TR might provoke the self-quenching of the probe. Self-quenching is manifested as a decrease in the fluorescence lifetime in addition to a reduction of fluorescence intensity. The degree of concentration for self-quenching highly depends on the quenching mechanism, which can occur via collisions between excited fluorophores, the formation of non-fluorescent dimers, or energy transfer to the non-fluorescent dimers. The discovery of the molecular mechanism yielding self-quenching of Flipper-TR is out of the scope of this work, but we investigated whether the lifetime of the probe was affected by a heterogeneous distribution along the membrane. For this, we measured the lifetime of Flipper-TR in supported lipid bilayers made of POPC with increasing concentrations of the probe (Figure 4A). Indeed, the lifetime of Flipper-TR decreased linearly with the concentration of the probe within the lipid bilayer as quantified by the fluorescence intensity (counts per pixel). From the linear fit, we could compare the theoretically predicted lifetime considering the concentration of self-quenching and the experimental value along the lipid bilayer of POPC GUVs or passive and active proteoGUVs (Figure 4B). Interestingly, whereas POPC and passive proteoGUVs displayed similar theoretical and experimental lifetimes, active membranes were characterized by experimental lifetimes lower than theoretically predicted (Figure 4C). This confirms that the rotational activity of ATP synthase unequivocally leads to a decrease in lateral pressure and lipid packing within lipid bilayers, independent of any potential quenching effects caused by the interaction of the probe with the protein.

ATP synthase modulates the elastic properties of plasma membrane in *Bacillus subtilis*

To gain deeper insight into how ATP synthase might modify the elastic properties of their host membranes in living cells, we tested the tension probe in *in vivo* models. Since gram-negative bacteria, such as *E. coli*, prevent the uptake of the tension probe due to their highly impermeable cell wall, we used the gram-positive *B. subtilis* as a suitable model for bacterium staining with Flipper-TR.[13] Bacteria display significant cell-to-cell heterogeneity in metabolism, which might impair the detection of membrane remodeling driven by the rotation of ATP synthase. To reduce the variability in ATP synthase activity among individual cells, the growth rate of cell culture was kept constant through serial dilutions (see methods). After at least two mass doubling steps, the cells were externally labeled with Flipper-TR, which clearly stained the plasma membrane and discerned the septum in dividing bacteria (Figure 5A).

Similar to GUVs and proteoGUVs, the fluorescence emission decay curves were fitted using three exponential components. Again, the reported lifetime corresponds to the longest component for the same reasons stated above. As a control, the basal packing state of the plasma membrane in *B. subtilis* was characterized by a lifetime of $\tau_1 = 4.6 \pm 0.1$ ns (29 images from $n = 4$ independent experiments), in agreement with data previously reported for gram-positive bacteria.[13] The high value for τ_1 might reflect the crowded environment of bacterial membranes.[14] The activity of ATP synthase was then modulated using specific drugs. First, cells were treated with the protonophore carbonyl cyanide m-chlorophenyl hydrazone (CCCP), which disrupts the proton gradient across the plasma membrane, thereby enhancing ATP synthase activity as an attempt to compensate for proton leakage.[15] Upon CCCP incubation, Flipper-TR showed a decrease in lifetime to $\tau_1^{CCCP} = 4.4 \pm 0.1$ ns (29 images from $n = 4$ independent experiments). However, the inhibition of ATP synthase with DCCD[11,12] did not alter the basal lifetime of untreated cells, $\tau_1^{DCCD} = 4.6 \pm 0.2$ ns (30 images from $n = 4$

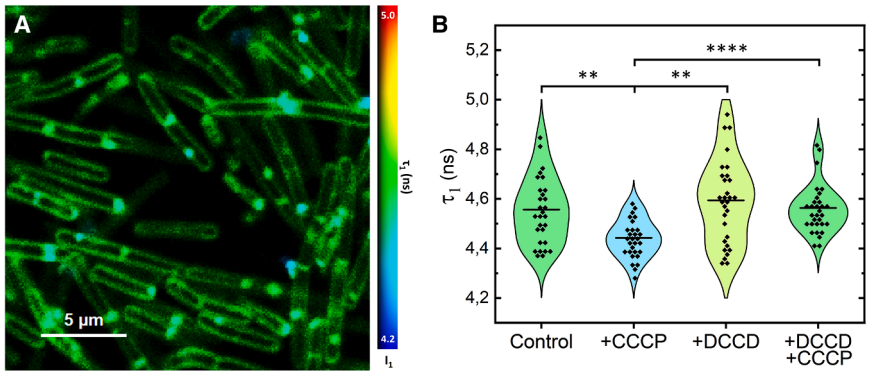

Figure 5. FLIM of *B. subtilis* labeled with Flipper-TR

(A) Fluorescence lifetime imaging of *Bacillus subtilis*. Scale bar, 5 μm.

(B) Violin plot of Flipper-TR lifetime, τ_1, of *B. subtilis* cultures upon incubation with different drugs: control (4.6 ± 0.1 ns, 29 images from n = 4), +CCCP (4.4 ± 0.1 ns, 29 images from n = 4), +DCCD (4.6 ± 0.2 ns, 30 images from n = 4), and +DCCD +CCCP (4.6 ± 0.1 ns, 31 images from n = 4). The mean is represented by a line. Mean values are expressed as the mean ± SD for N images from n independent experiments. Statistical significance: $^{**}p \leq 0.01$ and $^{****}p \leq 0.0001$.

independent experiments). Unlike in the *in vitro* experiments, Flipper-TR is not sensitive enough to detect the inhibited activity of ATP synthase in native membranes under the experimental metabolic state, possibly due to the crowded nature of the bacterial membrane. Interestingly, bacteria treated with both DCCD and CCCP also maintained the basal lifetime, $\tau_1^{CCCP+DCCD} = 4.6 \pm 0.1$ ns (31 images from $n = 4$ independent experiments), suggesting that this double treatment confirms that Flipper-TR is insensitive to changes in membrane potential, consistent with previous findings.[8] As DMSO (0.8% v/v) was used as a solvent for both CCCP and DCCD, control experiments were conducted with cells exposed to DMSO alone (0.8% v/v). Since the Flipper-TR lifetime remained unchanged over more than 60 min, we can rule out any significant impact of DMSO on the structural properties of the bacterial plasma membrane (Figure S5).

DISCUSSION

Active membranes are dynamic systems where embedded proteins or molecular motors, such as ATP synthase, actively generate forces that affect the membrane's mechanical properties and behavior.[16] In this context, the rotational movement of ATP synthase not only plays a vital role in energy production but also impacts the surrounding lipid bilayer, as shown in our findings. First, with micromanipulation experiments in a reconstituted system, we demonstrate that rotation reduces the membrane tension of the embedding lipid bilayer, which in turn leads to an apparent decrease in the membrane's bending modulus, as reported for other ion channels such as bacteriorhodopsin (BR)[17,18] and Ca^{2+} ATPase[19] using micropipette aspiration. Although we sometimes find heterogeneous protein distribution along the lipid bilayer (see Figures 2A and 3A) the micropipette aspiration technique inherently provides an ensemble-averaged measurement, where the elastic deformation occurs over a large membrane area, reducing the impact of local protein concentration variations. In addition, our experimental data show consistent bending rigidity values across multiple individual vesicles, indicating that protein clustering does not introduce significant variability. However, the protein density in our system remains low (from 10^{13} to 10^{14} proteins/m^2).[5] As changes in the lipid packing induced by protein activity are local,[6] the elastic remodeling observed here could be enhanced at higher intermediate protein densities. However, an extreme protein crowding, as seen in bacterial membranes, can lead to membrane rigidification and mask the observed effect.[20]

A decrease in membrane tension is often linked to enhanced membrane fluctuations observed in active membranes due to the forces generated by the embedded proteins. Initially modeled for ion channels, enhanced fluctuations are grounded on the forces generated by a change of conformation of the pumps, acting as force dipoles.[18] However, a direct link to relate the molecular effect of activity and the force generation remains elusive. Similar to BR,[18] Na^+ ATPase,[21] and K^+ ATPase,[20] ATP synthase also exhibits non-equilibrium membrane fluctuations,[5] but its force generation mechanism might rely on the rotational movement of the *c*-ring instead. We have proposed that the enhanced fluctuations in membranes containing rotors may result from local perturbations in lipid packing around the rotating proteins, a hypothesis supported by molecular dynamics simulations.[6] These coarse-grained simulations described an expansion of the acyl lipid chains under rotating conditions up to ≈7 nm away from the F_o proteins. Disruption of lipid packing reduces the membrane's overall tension, leading to increased flexibility and dynamic movement. However, direct experimental evidence linking these phenomena remained elusive.

Our results using FLIM with the fluorescent lipid tension reporter Flipper-TR in model membranes confirm that ATP synthase rotation leads to measurable changes in membrane properties, specifically, a reduction in the lipid packing density. Our experiments reveal that the spin movement of ATP synthase produces a significant decay in the lifetime decay of the tension probe from $\tau_1^{Passive} = 4.1 \pm 0.1$ ns to $\tau_1^{Active} = 3.8 \pm 0.3$ ns (Figure 2). Furthermore, Flipper-TR is insensitive to membrane potential,[8] which discards any side effect from the concomitant proton pumping of protein during ATP hydrolysis,[2] confirming that the membrane becomes less packed under rotational forces (Figure 6). However, the obtained FLIM data represent an ensemble-averaged measurement in both time and space along the membrane. The spatial resolution of fluorescence microscopy ranges from 100 to 200 nm, and images are taken at an approximate scan rate of 1 frame per second, a much slower timescale than protein dynamics. As a result, it is insufficient to capture a localized elastic remodeling.

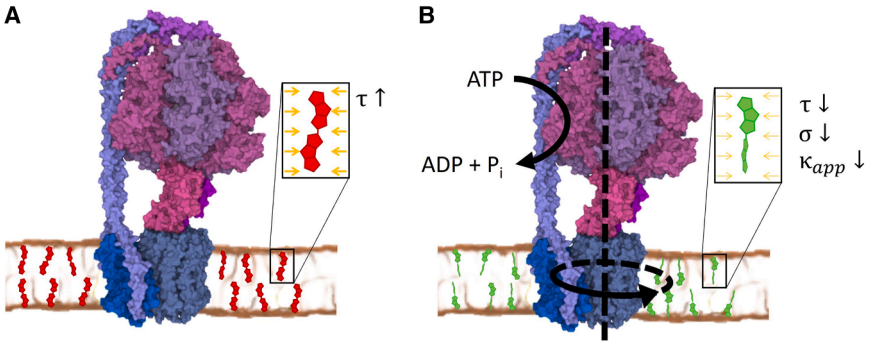

Figure 6. Elastic remodeling of lipid membranes by rotating ATP synthase as detected by Flipper-TR

In the absence of rotation (A), the lifetime value is high, corresponding to a basal packed state (red). Upon incubation with ATP, i.e., under active conditions (B), rotation of the *c*-ring lowers the lipid packing and the lateral pressure of the lipid membrane as reported by a decrease in the lifetime of the Flipper-TR probe (green). In consequence, the membrane tension, σ, is reduced and the apparent bending modulus, κ_{app} is decreased.

Still, our findings provide compelling evidence that rotation decreases the lateral pressure within membranes, altering their overall mechanical properties and potentially influencing a wide range of membrane-associated processes. In addition to enhanced membrane fluctuations,[5] protein rotation also drives the curvature sorting of ATP synthase into lipid nanofilaments.[6] The underlying mechanism for this curvature sorting is consistent with short-range, membrane-mediated protein-protein interactions, which are likely driven by changes in lipid packing in the immediate vicinity of the rotating proteins. These local perturbations in lipid organization might also play a crucial role in facilitating the self-assembly and spatial arrangement of proteins within real membranes.

Importantly, we extended these findings to living bacteria, demonstrating that ATP synthase modifies the elastic properties of native membranes, as detected by a change in the lifetime decay of Flipper-TR. However, biological membranes contain hundreds of lipid species and transmembrane proteins interacting and defining the membrane structure, organization, physical properties, and biological function. Thus, many other factors might play a role in membrane physical property modulation *in vivo*. In particular, the four-acyl-chain lipid cardiolipin (CL) shows a strong interaction with the F_o domain of ATP synthase.[22,23] A role as a lubricant has been suggested for CL,[24] providing this lipid with the potential capability of buffering the rotational effects within biological membranes. Moreover, bacterial cell membranes exhibit a high protein-to-lipid ratio (70/30 w/w),[14] which might impair the membrane-mediated interaction between rotating proteins. In particular, *B. subtilis* presents a dynamic and heterogeneous distribution of ATP synthase within the plasma membrane.[25] This discrete localization within the membrane might have an impact on the measurements by FLIM. Again, each data point represents an ensemble-averaged lifetime, whose value derives from all detected photons from different cells in a single field of view, effectively masking any molecular heterogeneities of the plasma membrane. Microenvironmental differences are not individually resolved but instead contribute to a smoothed, representative value. Nonetheless, dithienothiophene flippers[26] are fluorescent membrane probes with high mechanosensitivity,[8,27] characterized by partitioning into different membrane domains without strong specificity[27] while causing negligible disturbance to the surrounding membrane structure.[28] They also have shown a specific labeling of biological membranes[29] insensitive to membrane potential[8] and negligible fluorescence in water.[29,30] Flipper-TR is thus a tension probe that effectively detects changes in lipid packing in a biological context, underscoring the relevance of our results beyond model systems.

Overall, our results position ATP synthase rotation as a key modulator of membrane structure and dynamics. The rotational movement of ATP synthase, both *in vitro* and *in vivo*, reduces membrane tension, establishing a direct link between the protein's activity and the mechanical properties of the embedding membranes. The change in lateral pressure of membranes by the ATP synthase rotation may have important implications for the dynamic behavior of rotating proteins themselves, particularly in terms of their diffusion rates and mobility within membranes. Furthermore, understanding how rotating proteins impact phase-separated membranes could uncover new modulator roles for ATP synthase in lipid organization and cellular function. This may be especially significant in contexts where lipid heterogeneity is critical to biological processes in complex eukaryotic cells. Notably, the observed effects could be particularly relevant in mitochondrial membranes, where ATP synthase and CL are known to play a fundamental role in shaping the structure of cristae.[31] The precise molecular interactions between ATP synthase and the lipid bilayer in real biomembranes, as well as how the enzyme translates its rotary motion into membrane deformations, remain speculative, though,[32] and require further studies.

METHODS

Chemicals

Magnesium chloride ($MgCl_2$), sodium chloride (NaCl), potassium chloride (KCl), glucose, sucrose, tris(hydroxymethyl)aminomethane (Tris), adenosine 5′-triphosphate disodium salt (2Na^+ - ATP), DCCD, carbonyl cyanide m-chlorophenyl hydrazone (CCCP), bovine serum albumin (BSA), poly-L-lysine, and mineral oil were supplied by Sigma-Aldrich. n-dodecyl-β-d-maltoside (DDM) was purchased from VWR. Dimethyl sulfoxide (DMSO) was purchased from Fisher Scientific. Bacto tryptone and Bacto yeast extract were purchased from BD. Phosphate-buffered saline (PBS) was provided by GE Healthcare. Alexa 555-NHS was acquired from Thermo Fisher (Molecular Probes). Ultrapure

water was produced from a Milli-Q unit (Millipore, conductivity lower than 18 MΩ/cm).

Lipids

1,2-dioleoyl-sn-glycero-3-phosphoethanolamine-N-(7-nitro-2-1,3-benzoxadiazol-4-yl) (ammonium salt) (NBD-PC) and 1-palmitoyl-2-oleyl-sn-glycero-3-phosphocholine (POPC) were purchased from Avanti Polar. Flipper-TR was purchased from Spirochrome. Lipids were suspended in chloroform and stored at −20°C. Flipper-TR was suspended and aliquoted in DMSO and stored at −20°C.

Electroformation of GUVs

Giant vesicles were prepared using the standard electroformation protocol.[33] The fabrication chamber was composed of two 1-mm-spaced conductor indium tin oxide (ITO)-coated slides (7.5 × 2.5 cm^2; 15–25 Ω/sq surface resistivity; Sigma). Briefly, GUVs were prepared by transferring a volume of 10 μL of the POPC solution in chloroform (0.5 mg/mL) onto each ITO slide. For bending modulus experiment GUVs, the POPC solution was supplemented with 0.5%–3% mol NBD-PC. Samples were dried at room temperature and rehydrated in 200 mM sucrose, and the electrodes were connected to an AC power supply (10 Hz, 1.1 V; Agilent) for at least 3 h.

Protein purification and fluorescent labeling

Bacterial ATP synthase was purified from native *E. coli* MG1655 cytoplasmic membranes as described in Gutiérrez-Sanz et al.[34] and fluorescently labeled with fluorescent Alexa 555-NHS as described in Almendro-Vedia et al.[5] Labeled proteins were conserved in stock solution (200 mM sucrose, 10 mM KCl, 10 mM Tris-HCl [pH 8], and 0.5 mM DDM) at −80°C.

Protein reconstitution into GUVs

Protein reconstitution into GUVs was performed by mild detergent treatment with DDM.[35] Briefly, 0.4–1 μL of protein stock solution (≈0.2 mg/mL) was diluted with 10 μL of GUV solution and incubated for 45 min at room temperature. The DDM concentration was then below its critical micelle concentration (cmc_{DDM} = 0.17 mM), promoting protein incorporation in the membranous environment.

Micropipette aspiration experiments and bending modulus assay

The micromanipulation system consisted of a homemade micromanipulator using a pipette holder (Narishige) and a micrometer screw mounted on a vertical platform (ThorLabs). Borosilicate capillaries (0.5-mm inner diameter [ID] and 1-mm outer diameter [OD], World Precision Instruments) were pulled (PC-100, Narishige) and forged (MFG-5, Microdata Instruments) to form tips with 5–12 μm internal diameter. The micropipette was connected through the pipette holder to water tanks, and aspiration was controlled by hydrostatic pressure. The micromanipulation chamber was made up as previously reported.[6] The whole system was mounted on a Nikon Ti-E inverted microscope equipped with a Nikon C2 confocal scanning module, 488 and 561 nm continuous lasers (Sapphire), and a Plan Apo 100× NA 1.45 oil immersion objective (Nikon). Both the pipettes and the chamber were incubated with BSA (1 mg/mL) for 5 min at room temperature to inhibit strong adhesion of vesicles to the bottom of the observation chamber. After being washed, the chamber was filled with 200 mM salt buffer (15 mM HEPES [pH 7.4], 5 mM $MgCl_2$, 55 mM NaCl, and 100 mM glucose) and 10–20 μL of GUVs or proteoGUV solution. For active conditions, ATP was added (100 mM ATP, 100 mM potassium phosphate buffer [pH 7.2], and 100 mM $MgCl_2$) into the chamber buffer before manipulation to a final concentration of 1 mM. To avoid back-pressure effects from induced ΔpH and $\Delta\Psi$, both micropipette and FLIM experiments (see below) in GUVs lasted less than 30 min after the sample was incubated with ATP for every single data point. Both ΔpH and $\Delta\Psi$ reach steady values after 30 min of triggering the activity of the protein (see Almendro-Vedia et al.[5]). To measure the bending modulus with the micromanipulation device, a GUV is pulled out by a cylindrical micropipette in the aspiration mode.[36] The pressure difference, Δp, between the vesicle interior and the pipette determines the membrane tension, σ, as $\sigma = \Delta p \frac{R_p}{2}\left(1 - \frac{R_p}{R_V}\right)$, where R_p is the micropipette radius and R_V the vesicle radius. For a vesicle under suction at a given Δp, a protrusion length, L_p, is aspirated inside the pipette, and the relative excess area $\alpha = \frac{A - A_0}{A_0} = \frac{\Delta A}{A_0}$ is given by:

$$\alpha = \frac{\Delta L_p}{2R_p}\left[\left(\frac{R_p}{R_V}\right)^2 - \left(\frac{R_p}{R_V}\right)^3\right] \quad \text{(Equation 2)}$$

where ΔL_p is the variation in the protrusion length after applying a suction pressure, σ, and the protrusion length measured at the initial low tension, σ_0. For low tensions, the entropic regime dominates and the bending modulus is obtained from the linear fitting of the Canham-Helfrich equation, which connects the relative excess area α and the membrane tension σ through[7]

$$ln\left(\frac{\sigma}{\sigma_0}\right) \approx \frac{8\pi\kappa\alpha}{k_B T} \quad \text{(Equation 3)}$$

where κ is the bending modulus of the vesicle and $k_B T$ is the thermal energy.

Labeling of GUVs and proteoGUVs with Flipper-TR

Typically, 20 μL GUVs or proteoGUVs were diluted in 200 μL of buffer (10 mM HEPES [pH 7.2], 180 mM glucose, 100 μM $MgCl_2$, and 5 mM NaCl) and supplemented with the tension probe Flipper-TR at a final concentration of 1 μM for 15 min (typically 0.2 μL was added). For active conditions, ATP was added (100 mM ATP, 100 mM potassium phosphate buffer [pH 7.2], and 100 mM $MgCl_2$) to the observation chamber buffer before imaging to reach a final concentration of 1 mM. For non-hydrolyzable experiments, ADP was added (100 mM ADP, 100 mM potassium phosphate buffer [pH 7.2], and 100 mM $MgCl_2$) to the observation chamber buffer before imaging to reach a final concentration of 1 mM.

B. subtilis strain and growth conditions

B. subtilis ATCC 6051 was grown in LB medium and incubated aerobically overnight at 37°C in a shaking incubator and then

diluted 40 times. The optical density at 600 nm (OD_{600}) was measured periodically using an ultraviolet-visible (UV-vis) spectrophotometer (Genesis 10; Fisher Scientific) and always kept below 0.5 by serial dilutions (at least two) with pre-warmed medium for 5–6 h to increase the cell-to-cell homogeneity in metabolism.

Labeling of *B. subtilis* with Flipper-TR

Typically, 100 μL from the last diluted culture (at 0.3–0.5 OD_{600}) was centrifuged at 3,000 × *g* for 5 min at 25°C and resuspended into 100 μL of PBS supplemented with 0.2% (w/v) glucose. When required, bacteria were then incubated for 30 min at 37°C with 10 μM CCCP and/or 10 μM DCCD (final concentration). Both control and treated bacteria were exposed to 0.4% v/v DMSO at this incubation step. Bacteria were then transferred to a pre-poly-L-lysine-coated well and further incubated for 15 min at 37°C with Flipper-TR at a final concentration of 4 μM (0.8% v/v DMSO final concentration at imaging) (Figure S3).

FLIM

FLIM imaging was performed on a Nikon Eclipse Ti2 inverted microscope with the PicoQuant Upgrade Time Correlation Single Photon Counting (TCSPC) Kit (PicoQuant GmbH, Germany) adapted for time-resolved fluorescence measurements. Excitation at 485 and 560 nm was performed by a picosecond laser diode head LDH-D-C-485 and an LDH-D-TA-560C, respectively (PicoQuant GmbH, Germany), with an excitation rate of 20 MHz, and the emission signal was collected through a 600/50 nm band-pass filter. Samples incubated with Flipper-TR were analyzed with PicoQuant SymPhoTime 64 software (Fast FLIM; PicoQuant, Germany) using a multiexponential function with three lifetimes to fit nanosecond time-resolved decays. The weight of the each lifetime was quantified by the corresponding fractional intensity, as defined as $f_i = \frac{I_i}{I_t} = \frac{a_i\tau_i}{\sum_{i=1}^{3} a_i\tau_i}$. The third exponential was attributed to the experimental background and fixed during the fitting process. Lifetimes τ_1 and τ_2 were left free in all the analyses.

Spatial correlation between ATP synthase and Flipper-TR in proteoGUVs

To calculate the spatial correlation between the fluorescence intensities of Flipper-TR and ATP synthase in proteoGUVs, the fluorescence intensities of Flipper-TR (green channel) and ATP synthase (red channel) along the contour of the vesicles were linearized and correlated using a cross-correlation function in MATLAB R2023b.[6]

Flipper-TR in supported lipid bilayers

POPC lipids in chloroform were dried with a SpeedVac concentrator at room temperature and resuspended in distilled water to a final lipid concentration of 1 mg/mL. The lipid suspension was sonicated with a tip sonicator (Vibra-Cell 75115 Ultrasonic Liquid Processor) for 10 min in 5-min on-off cycles (40% power) to form unilamellar liposomes. Supported lipid bilayers (SLBs) were prepared in custom-made observation chambers (200 μL) on a thoroughly cleaned coverslip (Epredia 24 × 60 mm #1; 0.13–0.16 mm). The chamber was filled with 100 μL of a saline solution (100 mM NaCl and 150 mM $MgCl_2$) and 20 μL of small unilamellar vesicles (SUVs) of POPC (1 mg/mL) and incubated for 10 min. SLBs were washed out with buffer (10 mM HEPES [pH 7.2], 180 mM glucose, 100 μM $MgCl_2$, and 5 mM NaCl) and incubated with Flipper-TR at different final concentrations for 15 min at 25°C. The lifetime, τ_1, of Flipper-TR was plotted versus the concentration of the probe, as measured by counts/pixel. From the linear fit $\tau_1 = m \cdot I + b$, we obtained *m* and *b* parameters to calculate the theoretical lifetime at a given experimental intensity in other samples.

Statistical analysis

Bending modulus and lifetime values were tested via ANOVA. Differences among means were assessed using the Tukey mean difference test. Statistically significant difference was established as $^{*}p \leq 0.05$, $^{**} \leq 0.01$, $^{***}p \leq 0.001$, or $^{****}p \leq 0.0001$. The differences between the spatial correlation coefficients in the active and passive conditions were compared using t test.

RESOURCE AVAILABILITY

Lead contact

Requests for further information and resources and reagents should be directed to and will be fulfilled by the lead contact, Iván López-Montero (ivanlopez@quim.ucm.es).

Materials availability

This study did not generate new unique materials.

Data and code availability

- The data that support the findings of this study are available on request from the lead contact.
- This paper does not report original code.
- Any other additional information required to analyze the data reported in this paper is available from the lead contact upon request.

ACKNOWLEDGMENTS

This work was supported by grants PGC2018-097903-B-I00 (to I.L.-M. and M. P.L.) and PID2021-125024NB-C22 (to I.L.-M.) from *MCIN/AEI/10.13039/501100011033/* and *FEDER Una manera de hacer Europa*. D.V.G. thanks the Regional Government of Madrid for an assistant researcher contract (CT103/19/PEJ-2019-AI/IND-13687) and the Universidad Complutense de Madrid and Banco Santander for the PhD contract (CT58/21-CT59/21).

AUTHOR CONTRIBUTIONS

I.L.-M. conceived the original idea, designed the research, and acquired the funding; D.V.G. conducted the experiments; D.V.G., M.A.S., M.P.L., V.A.-V., and I. L.-M. analyzed data; B.O. and P.N. provided reagents and protocols; D.V.G. and I.L.-M. wrote the paper, and all the authors reviewed and edited the manuscript.

DECLARATION OF INTERESTS

The authors declare no competing interests.

SUPPLEMENTAL INFORMATION

Supplemental information can be found online at https://doi.org/10.1016/j.xcrp.2025.102567.

Received: October 15, 2024
Revised: February 17, 2025
Accepted: April 8, 2025
Published: April 30, 2025

REFERENCES

1. Davies, K.M., Anselmi, C., Wittig, I., Faraldo-Gómez, J.D., and Kühlbrandt, W. (2012). Structure of the yeast F_1F_o-ATP synthase dimer and its role in shaping the mitochondrial cristae. Proc. Natl. Acad. Sci. USA *109*, 13602–13607. https://doi.org/10.1073/pnas.1204593109.
2. Mitchell, P. (1966). CHEMIOSMOTIC COUPLING IN OXIDATIVE AND PHOTOSYNTHETIC PHOSPHORYLATION. Biol. Rev. *41*, 445–502. https://doi.org/10.1111/j.1469-185X.1966.tb01501.x.
3. Boyer, P.D. (1997). THE ATP SYNTHASE—A SPLENDID MOLECULAR MACHINE. Annu. Rev. Biochem. *66*, 717–749. https://doi.org/10.1146/annurev.biochem.66.1.717.
4. Senior, A.E. (1988). ATP synthesis by oxidative phosphorylation. Physiol. Rev. *68*, 177–231. https://doi.org/10.1152/physrev.1988.68.1.177.
5. Almendro-Vedia, V.G., Natale, P., Mell, M., Bonneau, S., Monroy, F., Joubert, F., and López-Montero, I. (2017). Nonequilibrium fluctuations of lipid membranes by the rotating motor protein F_1F_0-ATP synthase. Proc. Natl. Acad. Sci. USA *114*, 11291–11296. https://doi.org/10.1073/pnas.1701207114.
6. Valdivieso González, D., Makowski, M., Lillo, M.P., Cao-García, F.J., Melo, M.N., Almendro-Vedia, V.G., and López-Montero, I. (2023). Rotation of the *c* -Ring Promotes the Curvature Sorting of Monomeric ATP Synthases. Adv. Sci. *10*, 2301606. https://doi.org/10.1002/advs.202301606.
7. Evans, E., and Rawicz, W. (1990). Entropy-driven tension and bending elasticity in condensed-fluid membranes. Phys. Rev. Lett. *64*, 2094–2097. https://doi.org/10.1103/PhysRevLett.64.2094.
8. Colom, A., Derivery, E., Soleimanpour, S., Tomba, C., Molin, M.D., Sakai, N., González-Gaitán, M., Matile, S., and Roux, A. (2018). A fluorescent membrane tension probe. Nat. Chem. *10*, 1118–1125. https://doi.org/10.1038/s41557-018-0127-3.
9. Pécréaux, J., Döbereiner, H.-G., Prost, J., Joanny, J.-F., and Bassereau, P. (2004). Refined contour analysis of giant unilamellar vesicles. Eur. Phys. J. E *13*, 277–290. https://doi.org/10.1140/epje/i2004-10001-9.
10. Niggemann, G., Kummrow, M., and Helfrich, W. (1995). The Bending Rigidity of Phosphatidylcholine Bilayers: Dependences on Experimental Method, Sample Cell Sealing and Temperature. J. Phys. II France. *5*, 413–425. https://doi.org/10.1051/jp2:1995141.
11. Emling, F., and Holtje, J.-V. (1987). Autostimulation of Dihydrostreptomycin Uptake in Bacillus subtilis. Microbiology *133*, 3495–3504. https://doi.org/10.1099/00221287-133-12-3495.
12. Hermolin, J., and Fillingame, R.H. (1989). H+-ATPase activity of Escherichia coli F1F0 is blocked after reaction of dicyclohexylcarbodiimide with a single proteolipid (subunit c) of the F0 complex. J. Biol. Chem. *264*, 3896–3903. https://doi.org/10.1016/S0021-9258(19)84937-2.
13. Roffay, C., Manuel García-Arcos, J., Chapuis, P., López-Andarias, J., Schneider, F., Colom, A., Tomba, C., Meglio, I.D., Dunsing, V., Matile, S., et al. (2022). Technical insights into fluorescence lifetime microscopy of mechanosensitive Flipper probes. Preprint at bioRxiv. https://doi.org/10.1101/2022.09.28.509885.
14. Gennis, R.B. (1989). Biomembranes : Molecular Structure and Function, 1st edition (Springer-Verlag).
15. Hicks, D.B., Cohen, D.M., and Krulwich, T.A. (1994). Reconstitution of energy-linked activities of the solubilized F1F0 ATP synthase from Bacillus subtilis. J. Bacteriol. *176*, 4192–4195. https://doi.org/10.1128/jb.176.13.4192-4195.1994.
16. Prost, J., and Bruinsma, R. (1996). Shape fluctuations of active membranes. Europhys. Lett. *33*, 321.
17. Manneville, J.-B., Bassereau, P., Lévy, D., and Prost, J. (1999). Activity of Transmembrane Proteins Induces Magnification of Shape Fluctuations of Lipid Membranes. Phys. Rev. Lett. *82*, 4356.
18. Manneville, J.-B., Bassereau, P., Ramaswamy, S., and Prost, J. (2001). Active membrane fluctuations studied by micropipet aspiration. Phys. Rev. E *64*, 021908. https://doi.org/10.1103/PhysRevE.64.021908.
19. Girard, P., Prost, J., and Bassereau, P. (2005). Passive or Active Fluctuations in Membranes Containing Proteins. Phys. Rev. Lett. *94*, 088102. https://doi.org/10.1103/PhysRevLett.94.088102.
20. Aimon, S., Callan-Jones, A., Berthaud, A., Pinot, M., Toombes, G.E.S., and Bassereau, P. (2014). Membrane Shape Modulates Transmembrane Protein Distribution. Dev. Cell *28*, 212–218. https://doi.org/10.1016/j.devcel.2013.12.012.
21. Bouvrais, H., Cornelius, F., Ipsen, J.H., and Mouritsen, O.G. (2012). Intrinsic reaction-cycle time scale of Na+,K+-ATPase manifests itself in the lipid–protein interactions of nonequilibrium membranes. Proc. Natl. Acad. Sci. USA *109*, 18442–18446. https://doi.org/10.1073/pnas.1209909109.
22. Sobti, M., Walshe, J.L., Wu, D., Ishmukhametov, R., Zeng, Y.C., Robinson, C.V., Berry, R.M., and Stewart, A.G. (2020). Cryo-EM structures provide insight into how E. coli F1Fo ATP synthase accommodates symmetry mismatch. Nat. Commun. *11*, 2615. https://doi.org/10.1038/s41467-020-16387-2.
23. Corey, R.A., Song, W., Duncan, A.L., Ansell, T.B., Sansom, M.S.P., and Stansfeld, P.J. (2021). Identification and assessment of cardiolipin interactions with *E. coli* inner membrane proteins. Sci. Adv. *7*, eabh2217. https://doi.org/10.1126/sciadv.abh2217.
24. Duncan, A.L., Robinson, A.J., and Walker, J.E. (2016). Cardiolipin binds selectively but transiently to conserved lysine residues in the rotor of metazoan ATP synthases. Proc. Natl. Acad. Sci. USA *113*, 8687–8692. https://doi.org/10.1073/pnas.1608396113.
25. Johnson, A.S., van Horck, S., and Lewis, P.J. (2004). Dynamic localization of membrane proteins in Bacillus subtilis. Microbiology *150*, 2815–2824. https://doi.org/10.1099/mic.0.27223-0.
26. Chen, X., Bayard, F., Gonzalez-Sanchis, N., Pamungkas, K.K.P., Sakai, N., and Matile, S. (2023). Fluorescent Flippers: Small-Molecule Probes to Image Membrane Tension in Living Systems. Angew. Chem. Int. Ed. *62*, e202217868. https://doi.org/10.1002/anie.202217868.
27. Dal Molin, M., Verolet, Q., Colom, A., Letrun, R., Derivery, E., Gonzalez-Gaitan, M., Vauthey, E., Roux, A., Sakai, N., and Matile, S. (2015). Fluorescent Flippers for Mechanosensitive Membrane Probes. J. Am. Chem. Soc. *137*, 568–571. https://doi.org/10.1021/ja5107018.
28. Neuhaus, F., Zobi, F., Brezesinski, G., Dal Molin, M., Matile, S., and Zumbuehl, A. (2017). Correlation of surface pressure and hue of planarizable push–pull chromophores at the air/water interface. Beilstein J. Org. Chem. *13*, 1099–1105. https://doi.org/10.3762/bjoc.13.109.
29. Soleimanpour, S., Colom, A., Derivery, E., Gonzalez-Gaitan, M., Roux, A., Sakai, N., and Matile, S. (2016). Headgroup engineering in mechanosensitive membrane probes. Chem. Commun. *52*, 14450–14453. https://doi.org/10.1039/C6CC08771J.
30. Macchione, M., Chuard, N., Sakai, N., and Matile, S. (2017). Planarizable Push–Pull Probes: Overtwisted Flipper Mechanophores. Chempluschem *82*, 1062–1066. https://doi.org/10.1002/cplu.201600634.
31. Minauro-Sanmiguel, F., Wilkens, S., García, J.J., and Boyer, P.D. (2005). Structure of dimeric mitochondrial ATP synthase: Novel F 0 bridging features and the structural basis of mitochondrial cristae biogenesis. Proc. Natl. Acad. Sci. *102*, 12356–12358.
32. Almendro-Vedia, V., Natale, P., Valdivieso González, D., Lillo, M.P., Aragones, J.L., and López-Montero, I. (2021). How rotating ATP synthases can modulate membrane structure. Arch. Biochem. Biophys. *708*, 108939. https://doi.org/10.1016/j.abb.2021.108939.
33. Mathivet, L., Cribier, S., and Devaux, P.F. (1996). Shape change and physical properties of giant phospholipid vesicles prepared in the presence of an AC electric field. Biophys. J. *70*, 1112–1121. https://doi.org/10.1016/S0006-3495(96)79693-5.

34. Gutiérrez-Sanz, Ó., Natale, P., Márquez, I., Marques, M.C., Zacarias, S., Pita, M., Pereira, I.A.C., López-Montero, I., De Lacey, A.L., and Vélez, M. (2016). H_2-Fueled ATP Synthesis on an Electrode: Mimicking Cellular Respiration. Angew. Chem. Int. Ed. *55*, 6216–6220. https://doi.org/10.1002/anie.201600752.

35. Dezi, M., Di Cicco, A., Bassereau, P., and Lévy, D. (2013). Detergent-mediated incorporation of transmembrane proteins in giant unilamellar vesicles with controlled physiological contents. Proc. Natl. Acad. Sci. USA *110*, 7276–7281. https://doi.org/10.1073/pnas.1303857110.

36. Longo, M.L., and Ly, H.V. (2007). Micropipet Aspiration for Measuring Elastic Properties of Lipid Bilayers. Methods Mol. Biol. *400*, 421–437. https://doi.org/10.1007/978-1-59745-519-0_28.